American Economic Journal: Economic Policy 2018, 10(2): 90–116
https://doi.org/10.1257/pol.20150321

The Fall of Coal: Joint Impacts of Fuel Prices and Renewables on Generation and Emissions[†]

By Harrison Fell and Daniel T. Kaffine*

Since 2007, US coal-fired electricity generation has declined by a stunning 25 percent. Detailed daily unit-level data is used to examine the joint impact of natural gas prices and wind generation on coal-fired generation and emissions, with a focus on the interaction between gas prices and wind. This interaction is found to be significant. Marginal responses of coal-fired generation to natural gas prices (wind) in 2013 were larger, sometimes much larger, than the counterfactual with 2008 wind generation (gas prices). Additionally, these factors jointly account for the vast majority of the observed decline in generation and emissions. (*JEL* L94, L95, Q35, Q38, Q42, Q53)

The electricity generation profile of the United States has changed significantly over the last several years. Coal-fired generation, once representing a strong majority of US electricity generation, has declined approximately 25 percent from 2007 to 2013, reducing associated carbon dioxide emissions from coal by a substantial 500 million tons of CO_2 annually. At the same time, a dramatic decrease in natural gas prices, largely due to hydraulic fracturing extraction techniques, has led to substantial increases in gas-fired generation (Joskow 2013). Wind generation has also increased dramatically, driven by state-level renewable portfolio standards (RPS), federal production and investment tax credits, and technological advances (Schmalensee 2012). Clearly, these changes in coal, gas, and wind generation are related, but how? In terms of the impact on coal-fired generation, are there important interactions between wind and gas? Do these impacts vary across regions? How important has the decline in natural gas prices and the growth of wind been for the fall of coal? In this paper, we use plausibly exogenous daily variation in wind-generated electricity and fossil fuel prices to estimate their impacts, individually and jointly, on coal-fired generation and emissions. Our estimates increase our understanding of the recent remarkable decline in coal-fired generation.

* Fell: Department of Agricultural and Resource Economics, North Carolina State University, 2801 Founders Drive, Raleigh, NC 27695 (email: hfell@ncsu.edu); Kaffine: Department of Economics, University of Colorado Boulder, 256 UCB, Boulder, CO 80309 (email: daniel.kaffine@colorado.edu). We thank Erin Mansur, Meredith Fowlie, seminar participants at Colorado State University, 2014 CU Environmental and Resource Economics Workshop, 2015 Front Range Energy Camp, North Carolina State University, University of Colorado Boulder, University of Wyoming, and two anonymous referees for helpful comments. We thank ABB/Ventyx for data access via Velocity Suite.

† Go to https://doi.org/10.1257/pol.20150321 to visit the article page for additional materials and author disclosure statement(s) or to comment in the online discussion forum.

Our approach expands the literature in several key ways. First, we conduct our analysis across several Independent Systems Operator (ISO) regions, allowing us to examine varying effects by region, due to differing generation capacities, transmission possibilities, and regulatory regimes. Second, we use daily generation-unit level data, which allows us to exploit significant variation in fuel prices, load conditions, and wind generation. The use of this data does pose some challenges, namely dealing with the substantial number of days when generating units do not run, as well as accounting for possible response heterogeneity across the distribution of production levels. Thus, another contribution of this paper is that we apply recently developed censored quantile regression techniques and panel selection models to deal with these issues. Finally, we analyze the effects of increased renewable generation, falling natural gas prices, and interactions between these factors on the recent decline in coal-fired generation.

We find low natural gas prices and increased wind generation have both led to reductions in coal-fired generation and CO_2 emissions. Furthermore, the interaction between relative fuel prices (the coal-to-gas price ratio) and wind generation is statistically and economically significant in most regions. Due to this interaction effect, the marginal response to fuel prices is larger in magnitude under high levels of wind generation. The impact of the interaction effect is even more pronounced for wind—the marginal effect of wind generation is multiple times larger in magnitude in several regions under low natural gas prices. Across quantiles, we find heterogeneity in the marginal response to wind generation and fuel prices, with generally larger responses at lower quantiles. We also find that changes in relative fuel prices and wind generation jointly account for the majority of observed generation changes in the regions we examine, with falling natural gas prices having larger impacts than increased wind generation. Intensive margin responses (production decisions conditional on having positive production) play a larger role than extensive margin responses (the on/off decision).

Understanding changes in the generation mix of the electricity sector is important for several reasons. First, the electricity generation sector is an important anthropogenic source of local and global pollutants, such that even small changes in this sector may have profound impacts on total climate-related emissions and local air quality (Muller and Mendelsohn 2009, Jenner and Lamadrid 2013). This is shown in Figure 1, which displays the substantial decline in CO_2 emissions from the electricity sector relative to other sectors over the last decade. Second, while this decline is mainly attributable to the electricity sector, Figure 2 shows demand has played very little role. Instead, the shift out of coal toward wind and gas looks to be driving a large fraction of the decline in US CO_2 emissions. Given coal accounts for roughly 25 percent of US CO_2 emissions, understanding the evolution of coal-fired generation is a key and crucial aspect in terms of sources of carbon emissions and impact on global climate change.

Our findings contribute to a growing literature examining the impacts of renewables and low natural gas prices on the electricity generation sector. Many of these studies use simulated dispatch models over varying time horizons to determine both generation and capacity expansion in a variety of policy and market contexts (Denholm, Kulcinski, and Holloway 2005; Newcomer et al. 2008; and Fell

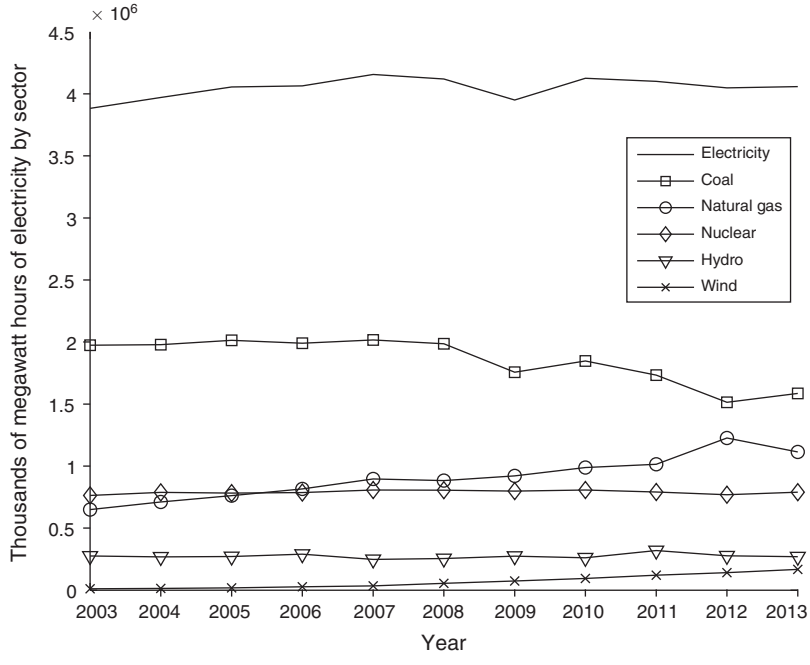

FIGURE 1. CO_2 EMISSIONS BY SECTOR

Source: EIA

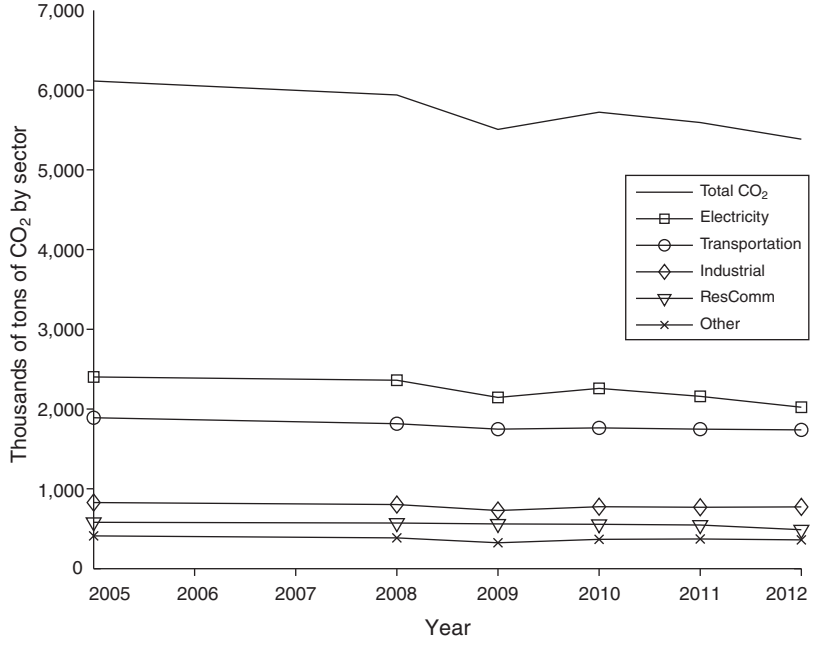

FIGURE 2. ELECTRICITY GENERATION BY SECTOR

Source: EIA

and Linn 2013). Recently, several studies have turned to observed data to determine how renewables (Cullen 2013; Kaffine, McBee, and Lieskovsky 2013; Novan 2015; and Callaway, Fowlie, and McCormick 2015) or low US natural gas prices (Lu, Salovaara, and McElroy 2012; Linn, Mastrangelo, and Burtraw 2014; Knittel, Metaxoglou, and Trindade 2015; Cullen and Mansur 2017; and Holladay and LaRiviere 2017) have affected existing generators and emissions, generally finding wind generation primarily displaces natural-gas-fired generation and that generation has shifted towards natural gas as prices have fallen.

It should be noted that we focus on the short-run operating decisions, or "operating margin," and discuss how wind generation and fuel prices affect these operating decisions below. Of course, low natural gas prices and increased wind generation may also impact the longer-run "build margin" or retirement decisions of coal plants. Given there has been relatively few retirements to date in the regions we examine, an empirical investigation of gas prices and wind generation on retirements of coal is left for future research. However, understanding these operating margin impacts are still of importance given the predicted significance of coal-fired generation as an electricity source for several years to come in the United States (35–40 percent of total net generation through 2030 per US Energy Information Agency's 2015 Annual Energy Outlook). In addition, understanding the interactions of increased wind generation and changes in relative fuel prices is important for understanding the outcomes from policy portfolios (e.g., the EU 20/20/20 Climate and Energy Package, or the US Clean Power Plan) that promote renewable energy and change the costs of burning coal relative to natural gas.

I. Background on Electricity Markets and Dispatch Curves

In this section, we provide some background on electricity markets, describe the pre-2008 view of the short-run supply curve, and motivate how the post-2008 fall in US gas prices and increase in wind generation affect coal-fired generation. The supply side of electricity markets is characterized by different generators with different fuel types and technologies, each with their own fixed capacities and marginal costs of generation. Ordering generators by marginal cost, the short-run supply or "dispatch" curve is a step-function characterized by discrete jumps in marginal cost. For any given level of demand in a competitive market, the lowest marginal cost generators are dispatched until the market clears, with the wholesale price of electricity determined by the marginal cost of the marginal generator. Those generators with marginal costs below the market-clearing marginal generator are thus inframarginal, while generators with higher marginal costs will simply not run. For inframarginal generators, the capacity factor (actual generation divided by potential generation) will be near one, while the marginal generator will typically operate at a capacity factor below one.

Consider a simplified dispatch model where the supply side consists of six generators, four coal and two gas. The coal generators are differentiated by their marginal cost, with two low-cost generators C_{L1} and C_{L2} and two high-cost generators C_{H1} and C_{H2}, and similarly for gas—G_L and G_H. Coal generators have a capacity of $0.5K$ and gas generators have a capacity of K. For simplicity, assume a constant

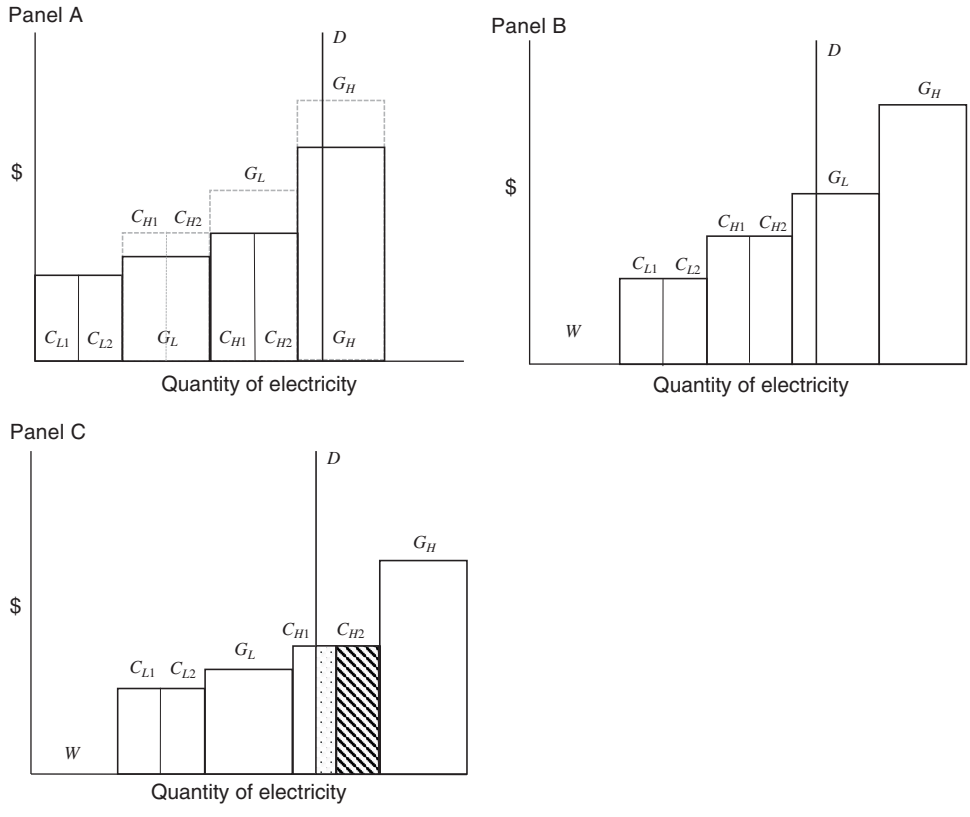

FIGURE 3. DISPATCH CURVE EXAMPLE

Notes: "*C*," "*G*," and "*W*" designate coal, gas, and wind units, respectively. Demand (load) is designated by "*D*." Panel A illustrates the effect of falling natural gas price in isolation. Panel B illustrates the effect of increased wind generation in isolation. Panel C illustrates the joint effect of falling natural gas prices and increased wind generation.

level of demand D, equal to $3.25K$, which could represent demand net of other zero marginal cost generators such as solar or must-run nuclear. Figure 3, panel A, illustrates this basic setup. The dashed gray lines represent the pre-2008 state of the world, where the highest-cost coal plants had lower marginal costs than the cheapest gas plant $(C_L < C_H < G_L < G_H)$. Given demand D, all coal plants are fully dispatched (capacity factor of 1). By contrast, only the low-cost gas plant is fully dispatched, with the high-cost gas plant operating at a capacity factor of 0.25. This setup matches the typical textbook discussion of electricity markets where coal plants supply low-cost "baseload," with higher cost gas plants used to meet "peak" demand.

However, post-2008 has witnessed a dramatic drop in US natural gas prices and a large increase in zero marginal cost wind generation. Figure 3, panel A illustrates the effect of the fall in natural gas price. While the low-cost natural gas plant G_L swaps position with the high-cost coal plants C_H in the dispatch curve, high-cost gas G_H remains the marginal generator, leading to no reduction in coal-fired generation. This is consistent with Cullen and Mansur (2017), whereby a small increase in the price of CO_2 would induce little coal-to-gas switching if future relative fuel prices

were similar to historic levels. Figure 3, panel B illustrates the effect of an increase in wind generation W. The marginal generator switches from high-cost gas G_H to low-cost gas G_L, but the same amount of coal-fired generation is produced. This is consistent with Cullen (2013), Kaffine, McBee, and Lieskovsky (2013), and Novan (2015), whereby only small amounts of coal are offset by wind generation in Texas in the mid- to late-2000s.

Figure 3, panels A and B considered the effect of a change in gas price and wind generation individually, with no resulting change in coal-fired generation. In panel C, gas price and wind generation changes are considered jointly. With a drop in gas price, the dispatch curve reorders (C_H and G_L swap) per Figure 3, panel A, followed by the increase in wind generation W per panel B. Now the marginal generator is high-cost coal C_{H1}, which runs at half capacity, while high-cost coal plant C_{H2} does not run at all, reducing the overall coal capacity factor from 1 to 0.625.[1]

While simplified, two points emerge that will be important for the empirical exercise that follows. First, the above example illustrates natural gas and wind may have complementary effects in terms of offsetting coal generation due to changes in the dispatch order. Furthermore, natural gas plants are generally better suited for ramping and quick adjustments to generation, while coal is designed for steady levels of constant generation. This may provide another channel by which increases in intermittent wind generation are paired with increased gas generation to handle the volatility of wind (Joskow 2011), at the expense of less-flexible coal generation.[2] Second, per Figure 3, panel C, the response by coal-fired generation has both an intensive (dotted area) and extensive margin component (hashed area). As such, while we first examine the intensive margin response of generation and emissions, it is important to note that the estimated response is not necessarily the overall effect.[3] We examine the extensive margin and total response to fuel prices and wind generation in detail at the end of the paper.

II. Data and Methods

A. *Data*

Our analysis employs daily, unit-level data. All data sources we use were made available to us by the energy data service company ABB via their Velocity Suite data management product, which organizes all publicly available datasets on electricity

[1] Throughout this simplified analysis we have assumed the marginal cost of the coal plants has remained the same, implicitly holding thermal efficiency constant. In practice, thermal efficiency may react to changes in the relative coal-to-gas prices and/or to wind generation. To the extent thermal efficiency does respond to fuel prices and wind generation and these responses subsequently impact capacity factors or emission rates, these efficiency improvements will be subsumed below in our empirically estimated coal-to-gas price ratio responses, wind generation responses, and/or time fixed effects.

[2] Dorsey-Palmateer (2014) finds evidence using data from Texas that increased wind generation shifts the fossil fuel generation mix toward natural gas generation, presumably to handle the intermittency of wind generation. Similarly, Baranes, Jacqmin, and Poudou (2015) finds evidence of complementarity in investment decisions that are attributed to intermittency considerations.

[3] For example, the change in average capacity factor for operating plants in Figure 3, panel C is relatively small. Furthermore, the median response in this example is actually zero, though lower quantiles would show more of a response.

generating facilities in a single searchable database. We begin by creating daily capacity factors and emissions for coal-fired generating units. The daily capacity factor measure, CF_{it}, is calculated as unit i's net generation (generation produced less power needed to operate the unit) on day t divided by its daily generating capacity, $CF_{it} = NetGen_{it}/GenCapacity_i$. The variable $NetGen_{it}$ is created by summing hourly gross generation (in megawatt hours—MWh) for a given day from EPA's Continuous Emissions Monitoring System database (CEMS) and adjusting for the ratio of net generation to gross generation using data from the NERC Generating Availability Data System (GADS). Daily generation capacity $GenCapacity_i$ is based on the given nameplate capacity (megawatt—MW) for each unit in the sample from the EIA 860 form, and is calculated as $GenCapacity_i = (nameplate\ capacity)_i \times 24$.

The CEMS database also includes hourly CO_2 emissions by unit and we use this to create our emissions variable.[4] The CO_2 emissions dependent variable, E_{it}, is a generation capacity-weighted measure, specifically $E_{it} = (CO_2)_{it}/GenCapacity_i$, where emissions of CO_2 are measured in tons/day. We use a generation capacity weighted emissions measure to directly remove the variation in emissions due to the size of the generating unit and to make parameters more interpretable across heterogeneously sized coal-fired units. Also, while net generation and CO_2 emissions are positively correlated, they are not perfectly correlated. For example, coal-fired units often need to be warmed up after a complete shutdown, and can thus create positive emissions without positive net generation.

The variables CF_{it} and E_{it} are formed for coal-fired units across the transmission regions of the Electric Reliability Council of Texas (ERCOT), Midcontinent Independent System Operator (MISO), PJM Interconnection, and Southwest Power Pool (SPP).[5] These ISOs were selected because they have publicly available data for daily wind generation, have significant coal generation, and capture nearly two-thirds of wind generation in the United States. Daily wind generation data was collected for each region over the period 2008–2013 and used to form W_t, which is the wind generation in hundreds of gigawatt hours (GWh) in the ISO of interest on day t.

The other key variable is the coal-to-natural gas price ratio for each unit, $P_{it}^R = P_{it}^C/P_{it}^G$, used to measure the relative effect of changes in natural gas prices. The coal price, P_{it}^C, is an ABB-modeled monthly estimate of the \$/MMBtu cost of coal for unit i based on running averages of publicly available delivered coal prices given in EIA 923 forms, and is therefore constant for all days t within a given month-year. This is not a major limiting factor as coal is typically contracted over

[4] Units subject to CEMS requirements are mandated to report continuous hourly emissions based on either direct gas measurements or continuous fuel feed monitoring and mass balance calculations. As noted in Kaffine, McBee, and Lieskovsky (2013) and Linn, Muehlenbachs, and Wang (2014), units below 25 MW capacity are not required to report, though these excluded generators are only a small percentage of the total market. The 25 MW minimum-capacity limit for CEMS means we drop 14, 5, 5, and 0 coal-fired units across MISO, PJM, SPP, and ERCOT, respectively.

[5] One possible concern of using ISO as the geographic region for our estimations is that ISOs import and export power out of their territory (Figure C.1). In robustness checks discussed below, we do consider specifications that control for the neighboring ISO's load and show the results from this specification are numerically similar to the results presented below.

Table 1—Data Summary

	ERCOT				MISO			
	Mean	SD	Mean-2008	Mean-2013	Mean	SD	Mean-2008	Mean-2013
CF	0.730	0.301	0.788	0.706	0.572	0.327	0.652	0.522
E	0.818	0.339	0.902	0.791	0.664	0.386	0.767	0.599
P^R	0.500	0.204	0.216	0.556	0.534	0.257	0.218	0.602
W	0.694	0.384	0.416	0.896	0.625	0.432	0.232	0.969
Load	278.198	85.918	268.226	286.543	83.524	56.691	84.428	85.154
	PJM				SPP			
CF	0.503	0.356	0.600	0.448	0.643	0.302	0.707	0.614
E	0.516	0.375	0.617	0.459	0.737	0.346	0.826	0.698
P^R	0.652	0.306	0.273	0.753	0.479	0.206	0.235	0.509
W	0.256	0.196	0.094	0.403	0.374	0.259	0.162	0.697
Load	210.488	136.731	218.142	207.795	54.245	39.563	53.025	56.441

Notes: Columns "Mean" and "SD" give the regional mean and standard deviation, respectively, of the variables over the entire sample. "Mean-2008" and "Mean-2013" give the regional mean of the variables for years 2008 and 2013, respectively. Units are in daily (MWhs of net generation)/(MWh of potential generation), daily (tons CO_2 emissions)/(MWh of potential generation), ($ per MMBtu of coal)/($ per MMBtu of natural gas), 100s of GWhs, and GWhs for *CF*, *E*, P^R, *W*, and *Load*, respectively.

relatively long periods and thus not volatile on a daily basis. The natural gas price P_{it}^G is modeled as the daily natural gas price ($/MMBtu) at the gas hub nearest to unit i, based on spot prices quoted by the Intercontinental Exchange (ICE). This provides a good measure of the price at competing natural gas plants in the vicinity of coal unit i. There is considerable heterogeneity in gas prices across hubs, thus P_{it}^G and P_{it}^R have considerable variation both temporally and cross-sectionally allowing for stronger identification. Across regions, 20–40 percent of the variation in fuel prices is unexplained by unit and season-by-year fixed effects, and about 50–75 percent of the variation in wind is unexplained by these fixed effects.

We also gathered several other key explanatory variables. To control for regional power demand (load), we collect the variable $Load_{it}$, which measures the power demanded (GWh) in unit i's "transmission zone" area on day t.[6] We also collect data on a unit's operating status and only include "operating" units.

The mean and standard deviation by ISO of the variables CF_{it}, E_{it}, P_{it}^R, W_{it}, and $Load_{it}$ are summarized over the entire sample in Table 1 under the columns "Mean" and "SD." The 2008 and 2013 mean values are also presented under columns "Mean-2008" and "Mean-2013." Average coal capacity factors and CO_2 emissions per unit of capacity have fallen from 2008 to 2013. At the same time, wind generation and the coal-to-natural gas price ratio have risen. However, mean load values have remained relatively constant.

[6] Transmission zones are ABB-created areas that, as stated in their documentation, "represent load pockets and these load pockets are derived through extensive analysis of FERC 714 data, ISO reports in ERCOT, WECC transmission cases, and Multiregional Modeling Working Groups (MMWGs) in the Eastern interconnect." Load for these areas is reported via data provided by the ISOs.

B. *Empirical Strategy*

There are several aspects of the relationship between coal-fired generation and emissions, relative fuel prices, and wind generation that we would like to uncover through our empirical analysis. First, we want to estimate the marginal response of capacity factor and emissions to P^R and W for each of the regions examined and to explore how these responses may have changed over time. Second, we want to estimate the marginal responses at different points across the distributions of our dependent variables to obtain a sense for how units operating in different market conditions respond to changing fuel prices and wind generation. Third, in addition to understanding how plants respond on the intensive margin to changes in relative fuel prices and wind generation, we want to also understand the extent to which these factors drive extensive margin responses. Finally, we want to know how the observed variation in P^R and W over our sample period has driven the substantial observed changes in coal-fired generation and emissions, in terms of both intensive and extensive margins. To accomplish these estimation goals we use two different estimation approaches—a censored quantile regression method to explore the intensive marginal effects and a Heckman two-step method to attribute overall impacts of fuel price and wind variation on the mean intensive and extensive changes in capacity factor and emission levels.

With respect to the quantile regression approach, the primary identification challenge in estimating the intensive-margin impacts of natural gas prices and wind generation on coal-fired units' daily capacity factors and emissions is that coal plants, for various reasons, do not generate power every day. While daily data allows us to exploit considerable variation in wind generation and natural gas prices, daily data also results in many "0" observations for the dependent variables. To obtain consistent parameter estimates $\boldsymbol{\beta}_\tau$ of the censored conditional quantile function for the τth quantile, $Q_{y_{it}}(\tau|\mathbf{X}_{it}) = \max(0, \mathbf{X}_{it}\boldsymbol{\beta}_\tau)$, we use the censored quantile estimation approach adapted to panel data models with fixed effects in Galvao, Lamarche, and Lima (2013)—henceforth, GLL. The GLL method is an update of the classic censored quantile regression approach developed in Powell (1986). More specifically, the Powell (1986) approach to obtaining unbiased estimates of β_τ in a censored quantile regression setting can be formulated for this particular application by choosing parameters to minimize the following:

$$(1)\quad Q(\boldsymbol{\beta}, \boldsymbol{\psi}, \boldsymbol{\kappa}, \boldsymbol{\omega}) = \frac{1}{N\overline{T}} \sum_{i=1}^{N} \sum_{t=1}^{T_i} \rho_\tau \Big[y_{it} - \max\Big(0, \beta_{1\tau} P_{it}^R + \beta_{2\tau}\big(P_{it}^R\big)^2 + \beta_{3\tau}\big(P_{it}^R\big)^3 + \beta_{4\tau} W_t + \beta_{5\tau} W_t^2 + \beta_{6\tau} W_t^3 + \beta_{7\tau}\big(W_t \times P_{it}^R\big) + \mathbf{x}_{it}'\boldsymbol{\psi}_\tau + \kappa_{i\tau} + \omega_{sy\tau}\Big)\Big].$$

In this specification, N is the number of cross-sectional units, $\overline{T}$ is the average number of observations per unit, T_i is the number of observations for unit i, $\rho_\tau(\cdot)$ is the standard loss function used in quantile regressions (i.e., the "check" function). We thus model y_{it}, the level of capacity factor or capacity-weighted emissions, as a flexible function of the ratio of coal to natural gas prices P_{it}^R, ISO-level wind

generation W_t, and the interaction of these two variables $\left(W_t \times P_{it}^R\right)$.[7] The vector $\mathbf{x}_{it}'$ includes other control variables such as regional load and load squared. Unit-level fixed effects are represented by κ_i, and ω_{sy} is the season-by-year fixed effect. Thus, identification is based on within season-year cross-sectional variation and from temporally within-unit variation. Regarding the exogeneity of W_t and P_{it}^R, although wind generation may be curtailed in response to demand conditions, we control for load and more generally find no significant relationship between daily load and wind generation. Over our sample, gas price variation is due largely to gas supply changes brought about by the plausibly exogenous shale gas boom, and gas is also storable and used in multiple sectors. Finally, coal procurement is generally contracted over relatively longer periods and can reasonably be considered fixed with respect to daily generation decisions.

While parameter estimates can be derived directly from minimizing (1), this approach is computationally difficult as the minimization is commonly hampered by a low frequency of convergence. However, as discussed in GLL, (1) is asymptotically equivalent to

$$
\begin{aligned}
(2)\quad Q(\boldsymbol{\beta}, \boldsymbol{\psi}, \boldsymbol{\kappa}, \boldsymbol{\omega}, \hat{\pi}) = \frac{1}{N\bar{T}} \sum_{i=1}^{N} \sum_{t=1}^{T_i} \rho_\tau \Big[& y_{it} - \beta_{1\tau} P_{it}^R + \beta_{2\tau} \left(P_{it}^R\right)^2 + \beta_{3\tau} \left(P_{it}^R\right)^3 \\
& + \beta_{4\tau} W_t + \beta_{5\tau} W_t^2 + \beta_{6\tau} W_t^3 + \beta_{7\tau} \left(W_t \times P_{it}^R\right) \\
& + \mathbf{x}_{it}' \boldsymbol{\psi}_\tau + \kappa_{i\tau} + \omega_{sy\tau} \Big] \mathbf{1}(\hat{\pi}_{it} > 1 - \tau + c_N),
\end{aligned}
$$

where $\mathbf{1}(\hat{\pi}_{it} > 1 - \tau + c_N)$ is an indicator function equal to one if $\hat{\pi}_{it} > 1 - \tau + c_N$ and 0 otherwise, $\hat{\pi}_{it}$ is a consistent estimate of the propensity score associated with being above the censoring point (i.e., unit i having positive net generation or CO_2 emissions on day t), and c_N is a user-defined constant set to $c_N = 0.05$ as in GLL (alternative constants yielded similar results). The estimation, therefore, is run on the subset of the observations which have an estimated propensity score greater than $(1 - \tau + c_N)$. Note, unlike the two-step Heckman-type model, this sample subset may include observations for which $y_{it} = 0$.

To obtain the sample subset on which to run the quantile regression, the first step is to obtain an estimate of the propensity score associated with having positive net generation or CO_2 emissions. To do this, we estimate a panel probit model using the method of Fernández-Val (2009), which also allows for fixed effects.[8] Defining z_{it}^* as the latent variable that, when greater than zero, leads unit i on day t to have a

[7] The cubic specification was chosen to provide an appropriately flexible response of the dependent variable to relative prices and wind levels. Robustness checks with linear and fourth-order polynomials in wind and relative prices yielded similar results and are further discussed below. We exclude higher polynomial terms of the interaction variable because much of the flexible response to wind and prices is picked up in the higher order W_t and P_{it}^R terms included. We also found higher order interaction terms were highly correlated with one another, presenting a possible multi-collinearity issue.

[8] The method of GLL allows for the formation of the propensity score through the estimation of nonparametric or an alternative parametric discrete-choice method. We adopted the probit estimation here as panel logit models in this application often failed to converge and because of its relative ease in implementation relative to nonparametric panel discrete choice methods.

positive capacity factor or positive emissions, then the latent regression representation of this discrete-choice model is

$$(3)\quad z_{it}^{*} = \gamma_1 P_{it}^{R} + \gamma_2 \left(P_{it}^{R}\right)^2 + \gamma_3 \left(P_{it}^{R}\right)^3 + \gamma_4 W_t + \gamma_5 W_t^2 + \gamma_6 W_t^3 + \gamma_7 \left(W_t \times P_{it}^{R}\right) + \mathbf{x}_{it}'\phi + \sum_{l=1}^{5} \kappa_l L_{it-l} + \alpha_i + \eta_{sy} + u_{it};$$

$$z_{it} = \begin{cases} 1 \text{ if } z_{it}^{*} \geq 0 \\ 0 \text{ if } z_{it}^{*} < 0 \end{cases}.$$

We again model this decision to run the unit as a flexible function of P_{it}^{R}, wind generation W_t, and the interaction of these two variables $\left(W_t \times P_{it}^{R}\right)$. The vector $\mathbf{x}_{it}$ controls for other relevant variables as described above. Unit-level fixed effects are captured in α_i, year-by-season fixed effects are accounted for in η_{sy}, and u_{it} represents the mean-zero disturbance term.

Note our specification of equation (3) also includes lagged load variables L_{it-l} (5 lags). Lagged load may affect z_{it} for several reasons, and we find several of the associated parameters are statistically significant across the regions and the F-statistic associated with the null that the associated parameters are jointly equal to zero is large and highly statistically significant in all regions.[9] Given the estimated parameters of equation (3), an estimated propensity score, $\hat{\pi}_{it}$, can be derived for each observation and that is used in the indicator function in (2). In our estimation of (2) and (3), standard errors are clustered at unit level to address serial correlation.

One difficulty in using this quantile method in a panel data setting is the interpretation of parameter estimate from the τth quantile given that the distribution of the dependent variable may be changing over time. To begin, recall this procedure recovers unbiased coefficient estimates of the censored conditional τth quantile function.[10] That is, conditional on the independent variables, the estimated function provides an estimate of the τth quantile. This is analogous to the output of an ordinary least squares (OLS) estimation, which provides a conditional expectations (i.e., conditional mean) function. And, just as the parameters of an OLS estimation can be used to derive marginal impacts on the conditional mean of the dependent variable, parameters from the quantile regression approach can be used to derive marginal impacts of independent variables on the τth conditional quantile of the dependent variable. In particular, we use the estimated parameters of this modeling framework to determine the marginal impact of changes in P^R and W along the intensive margin at various conditional quantiles and over a range of P^R and W values.[11]

[9] For example, coal units often shut down for extended periods for planned and unplanned maintenance, and these extended shutdowns are also likely associated with periods of reduced load as this reduces the opportunity cost of shutting down for maintenance.

[10] Note that while the GLL method imposes a data selection step, the parameter estimates derived are not solely relevant for selected data. Per GLL, the data selection step is part of the method for obtaining consistent parameter estimates for the censored conditional quantile function $Q_{y_{it}}(\tau | \mathbf{X}_{it}) = \max\left(0, \mathbf{X}_{it}\beta_{\tau}\right)$.

[11] This requires the values of P^R and W over which we are evaluating the marginal effects to lead to positive values of the dependent variable for the given quantile. Alternatively, if the values of P^R and W, along with the other

While it is of value to see how different parts of the conditional distribution respond to changes in relative fuel prices and wind generation, we are also interested in the marginal responses of the *expected* value of the dependent variables, conditional on the dependent variable being positive. Furthermore, we wish to determine how much of the observed variation in the means of CF and E over time can be attributed to the observed changes in P^R and W, via both intensive and extensive margin responses. Thus, we need an estimate of a conditional expectations function that is inclusive of the impact of P^R and W on the extensive operating margin (the on/off margin) and intensive margin. To obtain an estimate of such a conditional expectations function we estimate a Heckman two-step model, adapted to accommodate fixed effects in "large T" panel datasets as described in Fernández-Val and Vella (2011). Equation (3) is used for the selection step of this two-step method to determine the inverse Mills ratio (IMR) to be used in the intensity equation. For the intensity equation we again model the given dependent variable as a flexible function of P_{it}^R, wind generation W_t, and the interaction of these two variables $\left(W_t \times P_{it}^R\right)$ as in the quantile method.

More specifically, the intensity equation estimated is given as

$$(4) \quad y_{it} = \beta_1 P_{it}^R + \beta_2 \left(P_{it}^R\right)^2 + \beta_3 \left(P_{it}^R\right)^3 + \beta_4 W_t + \beta_5 W_t^2 + \beta_6 W_t^3 + \beta_7 \left(W_t \times P_{it}^R\right) + \theta \hat{\lambda}_{it} + \mathbf{x}_{it}' \psi + \kappa_i + \omega_{sy} + \epsilon_{it},$$

where $\hat{\lambda}_{it}$ is an estimate of the IMR derived from the estimation of the selection equation (3). Note this formulation of the selection equation and intensity equation allows for the selection step to be partially determined by variables that are excluded from the intensity equation, namely the lagged load variables L_{it-l}, which per the above discussion are significant determinants of z_{it}.

One concern regarding the exclusion restriction is that coal plants take some time (on the order of a day) to ramp from zero to positive production and that this ramping can be associated with excessive emissions or lower daily capacity factors following a start-up. In that case, it is possible that lagged load may impact y_{it} conditional on $y_{it} > 0$, and this would violate the exclusion restriction. For our application, this issue appears to have minimal impact for several reasons. First, ramping occurs rather infrequently—across regions we find that on average only about 1.5 percent (ERCOT) to 3.5 percent (PJM) of the days with $CF_{it} > 0$ were preceded by a day with $CF_{i,t-1} = 0$ (and similarly for emissions). Second, we considered several specifications to probe this issue further. Specifically, we estimate the two-step model using lagged load, but drop all observations y_{it} where $y_{it} > 0$ and $y_{i,t-1} = 0$, negating the impact of start-up ramping on our estimates. As an alternative check, we also drop $Load_{i,t-1}$ from the selection equation, as $Load_{i,t-1}$ in particular may violate the exclusion restriction due to the ramping timing. These models yield parameter estimates and marginal effects that are quantitatively very

dependent variables in $\mathbf{X}$, were such that the value of the conditional quantile function $\mathbf{X}_{it}\beta_\tau$ was negative, then the expected quantile value would be below the cutoff point (i.e., zero) and the marginal response would be zero.

similar to the results presented below, providing some evidence the ramping issue is not a critical concern for this particular application.

III. Results

In this section, we report estimates from the regression models described above. We begin by discussing our results pertaining to the intensive margin responses to relative fuel price changes and wind generation. This discussion is followed by results from our analysis that decomposes the observed changes in capacity factors over time due to relative fuel price changes, wind generation increases, and these two factors combined, which is inclusive of both intensive and extensive margin effects. All results presented are based on separately estimated quantile and Heckman two-step regression models for each ISO. We do a region-by-region analysis for two reasons. First, given different generation mixes and wind resource availability across ISOs, it is likely capacity factors and emissions would have different responses. Second, from a more practical standpoint, the size of the dataset with all ISO regions combined presented significant computational difficulties for both estimation procedures.

A. *Intensive Responses*

As noted above, we begin with a first-stage estimation of a discrete choice model on whether to run the unit or not on a given day. Results of the fixed effects probit estimation for the discrete choice model described in equation (3) are given in Tables A.1 and A.2 in online Appendix A and provide the basis for the propensity scores used in the second step of the quantile regressions and the derivation of the IMR in the Heckman two-step regressions.

Quantile Point Estimates and Marginal Effects.—Estimation results for the ISO-specific median quantile regressions (estimates of equation (2) with $\tau = 0.50$) using CF_{it} and E_{it} as dependent variables are given in Tables 2 and 3, respectively. Given the cubic form of equation (2), the marginal effects of relative fuel prices or wind generation are not readily apparent from these tables, however, many of the parameters are statistically significant. Importantly, we find the coefficient on the price-wind interaction term, $W \times P^R$, is negative (with the exception of MISO), implying a complementary relationship between low natural gas prices and high wind generation in terms of reducing coal-fired generators' capacity factors and CO_2 emissions. This interaction is also statistically significant across both dependent variable specifications and in all regions except MISO. The lack of significant interaction in MISO is likely due to the generation capacity mix in that region. More specifically, examining the ratio of combined cycle natural gas capacity to coal-fired generation capacity, we find MISO has the lowest ratio of the four regions at about 0.35 (versus roughly 0.4, 0.45, and 1.9 for PJM, SPP, and ERCOT), which may limit its ability to switch out of coal-fired generation. In addition, MISO has historically had a very high share of generation from coal-fired units (nearly 80 percent) relative to other regions, with very little generation coming from gas-fired units.

Table 2—Capacity Factor Results: Median Quantile

	ERCOT	MISO	PJM	SPP
P^R	0.354	0.290	−0.096	0.020
	(0.264)	(0.090)	(0.078)	(0.074)
$(P^R)^2$	−0.851	−0.766	−0.060	−0.134
	(0.351)	(0.136)	(0.067)	(0.067)
$(P^R)^3$	0.347	0.334	0.007	0.015
	(0.118)	(0.061)	(0.006)	(0.007)
W	0.007	−0.040	0.050	0.005
	(0.012)	(0.006)	(0.028)	(0.021)
W^2	−0.011	−0.002	0.090	0.021
	(0.015)	(0.011)	(0.046)	(0.031)
W^3	0.008	−0.003	−0.083	−0.018
	(0.005)	(0.003)	(0.037)	(0.015)
$P^R W$	−0.116	0.021	−0.157	−0.176
	(0.035)	(0.014)	(0.039)	(0.054)
Load	0.002	0.004	0.004	0.005
	(2.62e-04)	(0.001)	(3.59e-04)	(4.78e-04)
$Load^2$	−1.96e-06	−1.08e-05	−3.55e-06	−1.49e-05
	(3.61e-07)	(5.03e-06)	(5.06e-07)	(1.82e-06)
Observations	60,384	376,335	294,849	140,178
N	32	196	168	68

Notes: The dependent variable is capacity factor. "N" denotes number of cross-sectional units included in the quantile regression. Standard errors (SEs) are given in parentheses. SEs are clustered at the unit level. All specifications include unit-level and season-by-year fixed effects.

Table 3—CO_2 Emission Results: Median Quantile

	ERCOT	MISO	PJM	SPP
P^R	−0.096	0.320	−0.098	0.097
	(0.282)	(0.120)	(0.086)	(0.087)
$(P^R)^2$	−0.388	−0.805	−0.049	−0.215
	(0.342)	(0.183)	(0.073)	(0.075)
$(P^R)^3$	0.215	0.345	0.006	0.023
	(0.111)	(0.084)	(0.006)	(0.007)
W	−0.017	−0.051	0.046	−0.016
	(0.014)	(0.008)	(0.030)	(0.022)
W^2	−0.007	6.77e-04	0.035	0.011
	(0.018)	(0.013)	(0.052)	(0.041)
W^3	0.006	−0.004	−0.044	−0.015
	(0.007)	(0.004)	(0.041)	(0.021)
$P^R W$	−0.077	0.028	−0.118	−0.132
	(0.035)	(0.016)	(0.040)	(0.059)
Load	0.002	0.005	0.004	0.005
	(2.70e-04)	(0.001)	(3.62e-04)	(6.48e-04)
$Load^2$	−2.44e-06	−1.22e-05	−3.80e-06	−1.56e-05
	(3.82e-07)	(5.49e-06)	(4.91e-07)	(2.46e-06)
Observations	60,367	379,860	298,368	140,323
N	32	196	168	68

Notes: The dependent variable is CO_2 emissions per unit of capacity. "N" denotes number of cross-sectional units included in the quantile regression for year 2013. SEs are given in parentheses. SEs are clustered at the unit level. All specifications include unit-level and season-by-year fixed effects.

This suggests coal plants in MISO may be relatively more efficient compared to the natural gas units in that region.

The form of equation (2) implies that along the intensive margin, the marginal effects of P^R and W on the τth quantile of the dependent variable are given by

$$\frac{\partial y_{it}}{\partial P_{it}^R} = \beta_{1\tau} + 2\beta_{2\tau}P_{it}^R + 3\beta_{3\tau}\left(P_{it}^R\right)^2 + \beta_{7\tau}W_t; \tag{5}$$

$$\frac{\partial y_{it}}{\partial W_t} = \beta_{4\tau} + 2\beta_{5\tau}W_t + 3\beta_{6\tau}W_t^2 + \beta_{7\tau}P_{it}^R. \tag{6}$$

Marginal effects thus vary with the values of P^R and W. Note also the marginal effects are not a function of the selection indicator variable, as evaluating the marginal effects at different P^R and W levels does not imply the need to alter the subsample over which to estimate the τth quantile regression.

Given this form, we calculate "actual" and "counterfactual" marginal effects along the intensive margin for the capacity factor specifications (Table 4) and for the emissions specifications (Table 5). The actual marginal effects are based on using the given year's (2008 or 2013) ISO-specific average values of P^R and W in the marginal effects equations (5) and (6). In the counterfactual responses, for $\partial CF/\partial P^R$ we assume wind generation remains at its 2008 level and, likewise for $\partial CF/\partial W$, P^R is held at its 2008 average value. Thus, the 2013 rows give us a measure of the marginal effects of P^R and W given their actual 2013 averages, as well as a measure of what the marginal effects would have been had P^R or W remained at their relatively low 2008 levels.

The results presented in Table 4 display several readily apparent features. First, most of the marginal effects are statistically significant.[12] Second, in all regions, the median marginal effects of P^R and W become more negative from 2008 to 2013. In part, this reflects the fact that across the ISOs, the marginal effect of P^R on CF becomes more negative as the coal-to-natural gas price ratio increases from 2008 to 2013 levels. This marginal effect also becomes more negative due to the fact that from 2008 to 2013, wind generation increased in all regions, and all regions (except MISO) have a negative parameter on the interaction term $W \times P^R$. A similar line of reasoning explains why the marginal effect of W on CF became more negative from 2008 to 2013.

Finally, the "counterfactual" marginal effects in 2013 are generally of smaller magnitude than the 2013 "actual" marginal effects, with the previously noted exception of MISO. Indeed, in some of these regions the disparity between the counterfactual and actual marginal effects is quite large. For instance, in ERCOT, the marginal effect of wind generation W on capacity factor based on 2013 average values of W

[12] The SEs of the marginal effects are calculated based on treating the marginal effects as linear functions of normally-distributed parameter estimates. Alternatively, one could bootstrap the SEs for the marginal effects. However, given the large sample sizes, this was not feasible for all regions. We did calculate the bootstrapped SEs of the marginal effects for ERCOT and SPP, and the bootstrapped SEs were smaller than those presented here.

Table 4—Quantile Median Marginal Effects for Capacity Factor

	ERCOT	MISO	PJM	SPP
Panel A. $\frac{\partial CF}{\partial P^R}$				
2008 Actual	−0.014	0.009	−0.142	−0.069
	(0.128)	(0.043)	(0.045)	(0.041)
2013 Actual	−0.374	−0.248	−0.238	−0.227
	(0.072)	(0.026)	(0.024)	(0.032)
2013 Counterfactual	−0.318	−0.264	−0.190	−0.133
	(0.064)	(0.025)	(0.023)	(0.020)
Panel B. $\frac{\partial CF}{\partial W}$				
2008 Actual	−0.023	−0.036	0.022	−0.032
	(0.008)	(0.004)	(0.016)	(0.013)
2013 Actual	−0.059	−0.040	−0.036	−0.083
	(0.007)	(0.004)	(0.008)	(0.012)
2013 Counterfactual	−0.019	−0.048	0.039	−0.034
	(0.012)	(0.009)	(0.016)	(0.021)

Notes: "2008 Actual" and "2013 Actual" are marginal effects calculated using 2008 or 2013 variable averages. "2013 Counterfactual" in panel A holds W at 2008 averages and in panel B holds P^R at 2008 averages in the calculation of the marginal effects. Standard errors are given in parentheses below the estimated marginal effects.

Table 5—Quantile Median Marginal Effects for CO_2 Emissions

	ERCOT	MISO	PJM	SPP
Panel A. $\frac{\partial E}{\partial P^R}$				
2008 Actual	−0.265	0.025	−0.135	−0.022
	(0.144)	(0.057)	(0.049)	(0.053)
2013 Actual	−0.397	−0.248	−0.210	−0.196
	(0.049)	(0.031)	(0.023)	(0.038)
2013 Counterfactual	−0.360	−0.269	−0.173	−0.126
	(0.040)	(0.032)	(0.025)	(0.028)
Panel B. $\frac{\partial E}{\partial W}$				
2008 Actual	−0.036	−0.045	0.019	−0.045
	(0.008)	(0.005)	(0.017)	(0.015)
2013 Actual	−0.058	−0.045	−0.036	−0.090
	(0.009)	(0.005)	(0.008)	(0.012)
2013 Counterfactual	−0.032	−0.056	0.021	−0.054
	(0.012)	(0.010)	(0.018)	(0.023)

Notes: "2008 Actual" and "2013 Actual" are marginal effects calculated using 2008 or 2013 variable averages. "2013 Counterfactual" in panel A holds W at 2008 averages and in panel B holds P^R at 2008 averages in the calculation of the marginal effects. Standard errors are given in parentheses below the estimated marginal effects.

and P^R is approximately triple what it would be in the counterfactual where natural gas prices remained at its high 2008-average level. Similarly, in SPP, the marginal effect of P^R on CF based on the 2013-average values of W and P^R is about 55 percent larger than what it would have been in the counterfactual where wind generation remained at its low 2008-average level.

The marginal effects at various price ratio and wind generation levels are shown in Figures 4 and 5, which give the marginal effect of P^R and W on CF over a range

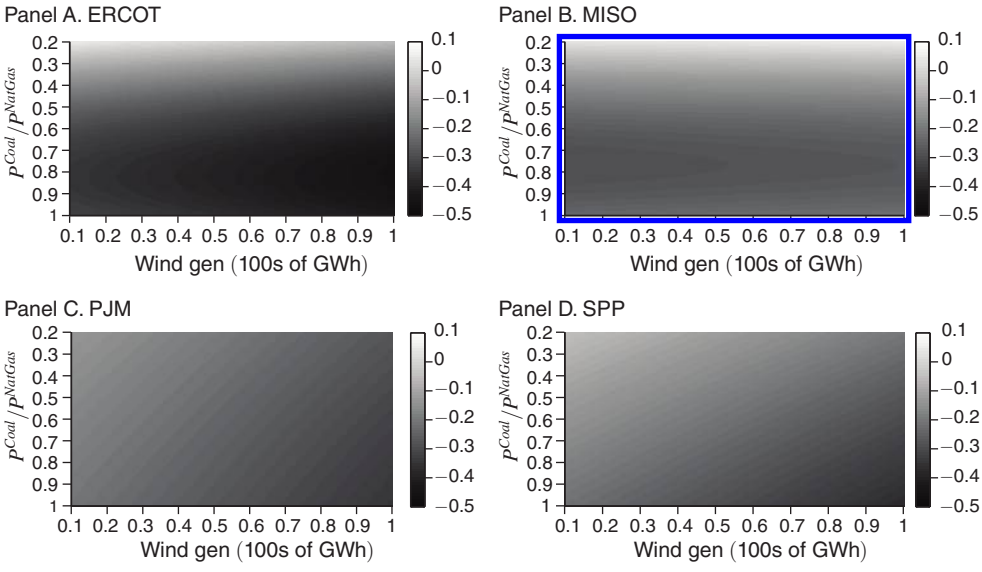

FIGURE 4. MEDIAN QUANTILE MARGINAL EFFECTS—$\frac{\partial CF}{\partial P^R}$

of values in the form of a "heat map."[13] Roughly speaking, values in the upper left corner correspond to 2008 levels of prices and wind, while values in the lower right corner correspond to 2013 levels. In Figure 4, we show for a given P^R value, the marginal effect of P^R increases in magnitude as the wind generation level increases for ERCOT, PJM, and SPP. On the other hand, results from MISO in Figure 4 show that while the marginal response of CF to P^R generally increases as P^R increases, these responses appear to remain constant as W increases.

In Figure 5, the marginal response of CF to W generally increases in magnitude as P^R increases across regions, again with the exception of MISO. The P^R and W values in 2008 again correspond to the area in the upper left corner, where we find very little response of capacity factors, and therefore CO_2 emissions, to wind generation (see Figures C.3 and C.4 in online Appendix C for similar marginal CO_2 responses). However, by 2013, P^R and W values are now in the lower right corner, and the larger response by coal generators highlights the importance of considering both fuel price ratios *and* wind generation levels.

Turning to the estimated marginal effects on emissions, shown in Table 5, we find the results follow the same basic patterns as those described above for CF. Again, largely significant marginal effects that become more negative from 2008–2013, and actual marginal effects that are more negative than the counterfactual effects. This is as expected given the correlation between capacity factors and CO_2 emissions per unit of capacity.

[13] The range of P^R and W displayed in these figures generally fall within the first to ninety-ninth percentiles of the observed daily data for all regions. The exception to this are for W, where the first percentile is slightly positive (in the range of 0.02 to 0.076 across regions) and for W in PJM, where the ninety-ninth percentile of wind is just above 0.8. The data also cover the full variable space, with the exception of the far upper-right corner of PJM.

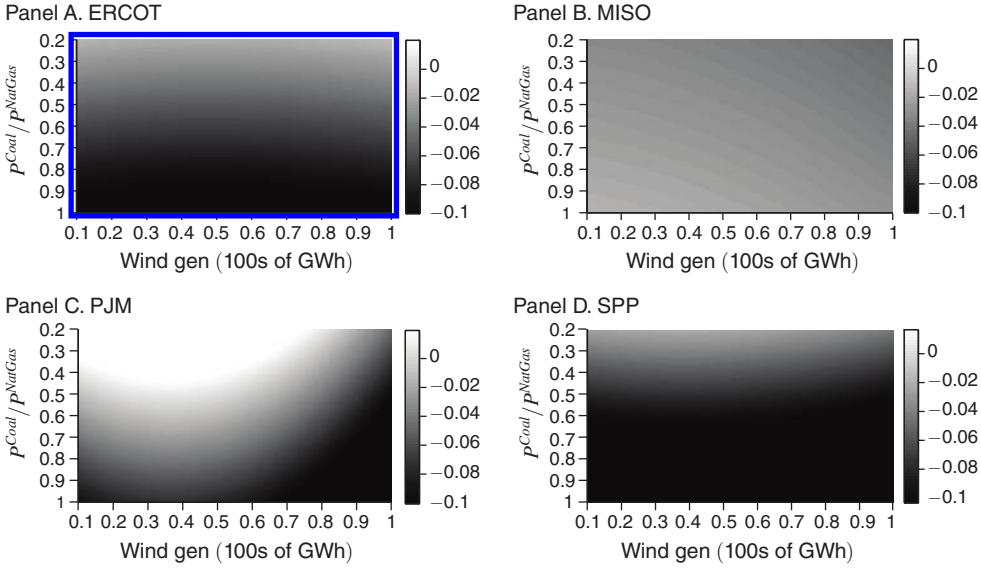

FIGURE 5. MEDIAN QUANTILE MARGINAL EFFECTS—$\frac{\partial CF}{\partial W}$

Comparing with prior literature, the response of coal to fuel prices is consistent with Cullen and Mansur (2017), who show decreasing the relative price of natural gas decreases CO_2 emissions (via reduced coal generation) at an increasing rate.[14] The results for wind shown in Figure 5 for ERCOT also largely confirm what has been found in Cullen (2013), Kaffine, McBee, and Lieskovsky (2013), and Novan (2015). These papers find little response of emissions to wind generation among coal plants in ERCOT using data from the mid- to late-2000s. By contrast, our results that wind generation offsets more emissions from coal generators in the low gas price environment are somewhat at odds with Holladay and LaRiviere (2017), who find wind generation generally offsets less emissions from the electricity sector under lower natural gas prices. Pinning down why their results are different is difficult given the substantial differences in approaches. One key difference in approach is that they use aggregated regional data instead of plant level data and do not directly estimate generation or emission responses to fuel prices or renewable generation. Their simulated responses to wind may therefore be missing key wind-gas price interaction aspects that we more fully account for in this study.

Heterogeneity across Quantiles.—We next examine how the marginal effects vary across quantiles. These comparisons are given in Table 6 for the *CF* specifications and in Table 7 for the *E* specifications. The tables present the marginal effects for each region based on 2013-average values for P^R and W for quantile levels of

[14] In considering these comparisons, it is important to recall that our estimates reflect marginal quantile responses along the intensive margin, as opposed to average treatment effects encompassing both intensive and extensive margin responses. Nonetheless, the qualitative conclusions are similar.

Table 6—Quantile Comparison for Capacity Factors

Quantile	ERCOT	MISO	PJM	SPP
Panel A. $\frac{\partial CF}{\partial P^R}$				
0.25	−0.597	−0.253	−0.133	−0.391
	(0.078)	(0.042)	(0.035)	(0.087)
0.50	−0.374	−0.248	−0.238	−0.227
	(0.072)	(0.026)	(0.024)	(0.032)
0.75	−0.222	−0.202	−0.210	−0.180
	(0.052)	(0.020)	(0.018)	(0.025)
Panel B. $\frac{\partial CF}{\partial W}$				
0.25	−0.077	−0.059	−0.015	−0.094
	(0.010)	(0.008)	(0.019)	(0.023)
0.50	−0.059	−0.040	−0.036	−0.083
	(0.007)	(0.004)	(0.008)	(0.012)
0.75	−0.035	−0.030	−0.026	−0.056
	(0.007)	(0.003)	(0.005)	(0.007)

Note: Standard errors are given in parentheses below the estimated marginal effect.

Table 7—Quantile Comparison for Emissions

Quantile	ERCOT	MISO	PJM	SPP
Panel A. $\frac{\partial E}{\partial P^R}$				
0.25	−0.554	−0.275	−0.105	−0.354
	(0.069)	(0.048)	(0.035)	(0.085)
0.50	−0.397	−0.248	−0.210	−0.196
	(0.049)	(0.031)	(0.023)	(0.038)
0.75	−0.272	−0.214	−0.189	−0.161
	(0.042)	(0.023)	(0.019)	(0.036)
Panel B. $\frac{\partial E}{\partial W}$				
0.25	−0.078	−0.066	−0.019	−0.086
	(0.011)	(0.009)	(0.017)	(0.022)
0.50	−0.058	−0.045	−0.036	−0.090
	(0.009)	(0.005)	(0.008)	(0.012)
0.75	−0.043	−0.034	−0.025	−0.067
	(0.007)	(0.004)	(0.005)	(0.009)

Note: Standard errors are given in parentheses below estimated marginal effect.

0.25, 0.50, and 0.75.[15] For the capacity factor and emissions responses with respect to P^R, in ERCOT and SPP the magnitude of the marginal response is substantially larger, and statistically different, at the lower quantiles. We may expect such a result if less efficient units are more likely to represent lower percentile observations and are thus more likely to run at reduced capacity factors with falling natural gas prices. Lower percentile observations are also likely to include observations with lower net load (load net of non-dispatchable and must-run generation), and this would

[15] We chose to examine a minimum of the twenty-fifth quantile because examining quantiles below this would result in expected quantile values at the zero cutoff value. We also examined quantiles above the seventy-fifth quantile shown here. The results were numerically and statistically similar to the seventy-fifth quantile results.

also increase the likelihood a coal unit would run at reduced capacity factors as gas prices fall. While MISO follows a similar pattern, the differences across quantiles are not nearly as large. This lack of differentiated responses across the quantiles could be caused by many factors. For instance, if the marginal costs of generation for coal units in MISO are quite similar, then the impacts of falling gas costs may be shared across more units, creating a more equalized response across quantiles.

The most interesting case is PJM, which looks similar to other regions at the fiftieth and seventy-fifth quantiles, but has a much *smaller* response at the twenty-fifth quantile. PJM has the lowest capacity factor, conditional on operating, of all the regions examined (64 percent on average in 2012). As such, the attenuated marginal effect at the twenty-fifth quantile may reflect the technical constraint that, conditional on operating, coal plants cannot operate below around 40 percent capacity factor, constraining the scope for a response to changing market conditions (Fell and Linn 2013).

With respect to the marginal responses to wind generation, the results are more similar across the regions. In general, for both the capacity factor and emission specifications, we find the marginal response to wind generation at the twenty-fifth quantile is generally 1.5–2 times larger in magnitude and statistically different than at the seventy-fifth quantile, again with the exception of PJM. Again, we would expect the response to be larger in magnitude at the lower quantiles to the extent lower quantile observations represent less favorable operating conditions. In addition, as adding wind generation to the system imposes a technical constraint of balancing power generation and power consumption that is common to all regions, it is also not surprising we find a more similar pattern of responses across the quantiles in each of the regions examined.

Heckman Model Results.—We also derive marginal effects on the intensive-margin from the Heckman two-step estimation. These estimates provide an average marginal effect, as opposed to the quantile-specific marginal responses discussed above. Full results and discussion of the marginal effect derivation are available in online Appendix A (Tables A.3–A.5); however, we highlight a few key points comparing results from this model with the quantile estimates. First, for capacity factors we again find ERCOT, PJM, and SPP have a negative interaction effect between wind generation and fuel price ratio and that it is statistically significant for ERCOT and SPP (the p-value on the interaction parameter is 0.12 in PJM). For CO_2 emissions per unit of capacity, the parameter estimates again show a negative interaction effect in ERCOT, PJM, and SPP, though it is only statistically significant in ERCOT. Second, marginal effects generally follow the magnitude and pattern of the median quantile regression estimates, with the magnitude of marginal effects increasing from 2008 to 2013, with the notable exception of PJM. The smaller-magnitude of the average marginal response in 2013 for PJM is consistent with the result from the twenty-fifth quantile estimation, which suggested that technical constraints may be limiting the response for observations at lower quantiles of the capacity factor distribution. Overall, the results from the Heckman two-step method provide further evidence of the robustness of our general finding of a significant interaction effect, as well as to the approximate size of this effect and the intensive margin effects.

B. *Robustness Checks and Discussion*

We considered several variations of the quantile model described above. First, one might be concerned load outside of a unit's given ISO might affect generation decisions, so we considered specifications where we included external loads as controls. Likewise, we considered specifications where we controlled for wind generation outside of the given ISO. We also considered specifications where we altered the polynomial order of the P^R and W terms. Finally, we also consider specifications that allow us to more fully exploit the hourly nature of the generation, load, and wind generation data. More specifically, we replace daily wind generation variables in equations (2) and (3) with the day's average hourly wind-to-load ratio. This specification attempts to account for how significant wind generation is relative to load in a given day. We also consider specifications where we aggregate capacity factors, emissions, load, and wind generation across peak hours (hours beginning 8:00 AM–7:00 PM) and off-peak hours (hours beginning 12:00 AM–7:00 AM and 8:00 PM–11:00 PM). Results from these alternative specifications are given in online Appendix B. Most results are quite similar to those presented in our baseline specifications, and in particular, there is a similar general result of a negative and statistically significant interaction effect in all areas except MISO.

We also estimated models where instead of using $Load_{it}$ as an independent variable, we included transmission zone electricity prices, $pricemwh_{it}$. As this is likely to be endogenous due to simultaneity bias, we instrumented for $pricemwh_{it}$ with $Load_{it}$ and $Load_{it}^2$. Parameter estimates and marginal effects were similar to those above. Because we are using data at the generating unit level, we also considered specifications that allowed coal-fired units in plants that also had natural gas-fired units to have a different response from those units in plants with only coal-fired units. Results from this specification did show units in plants that also have natural gas-fired units are somewhat more responsive to P^R and W. However, the differences between the responses of these two groups were not significantly different from one another and marginal effects were not materially different from what is shown here.

Relating our intensive margin estimates back to Figure 3, note that this figure represents a snapshot of the electricity market at a particular point in time. Since the markets clear throughout the day as demand varies, the marginal unit will vary across the day. Mapping this to the daily data used in this analysis, this market clearing process gives rise to a conditional distribution of CF (or E) across observations (conditional on $CF > 0$ for the day), where units with lower daily CF are closer to the margin more often throughout the course of the day, while units with higher CF are typically less often near the margin.[16] Recall that the dotted area (or more precisely its width) in Figure 3 reflects the intensive margin response to wind/fuel prices. Then the conditional expectation estimates (Heckman model) captures how the mean of the CF distribution shifts in response to wind/fuel prices, which can

[16] Note that because coal plants cannot start up instantly after shutting down, a coal unit may also be "off the margin" and still have positive production. In this case, a coal unit may ramp down to its min-run level (typically 40 percent of capacity) then ramp back up as it becomes marginal or inframarginal. The reduction in CF when a unit is pushed off the margin, but is still running, would be captured in the intensive margin estimates, represented in Figure 3 by a dotted bar.

Table 8—Predicted Average Propensity Scores for Capacity Factor

	ERCOT	MISO	PJM	SPP
2008	0.919	0.890	0.889	0.900
2009	0.889	0.817	0.807	0.875
2010	0.908	0.848	0.820	0.881
2011	0.922	0.810	0.783	0.869
2012	0.844	0.726	0.689	0.804
2013	0.894	0.748	0.686	0.822

Note: Values above are the predicted average propensity scores $\hat{\pi}$ for capacity factor by region by year from equation (3).

be thought of as the dotted area averaged over all hours and all units. Similarly, the conditional quantile estimates captures how the specified quantile of the *CF* distribution shifts, which can be thought of as the dotted area averaged over all hours for the specified quantile.

Finally, it is important to recall that the quantile results described above pertain solely to the intensive margin responses of operating plants. To get a sense of the extensive margin responses, Table 8 displays the estimated propensity score $(\hat{\pi})$ by region by year for capacity factor. While the estimated average probability of a plant operating is fairly similar across regions in 2008 (about 90 pecent), and all regions exhibit a generally declining propensity score over time, PJM has the most dramatic decline in predicted propensity score, followed by MISO. This suggests that extensive margin responses may play a larger role in PJM, and to a lesser extent MISO, than in ERCOT or SPP. While these values provide some context regarding potential extensive margin responses, note that the estimated propensity scores embed changes in other variables over time, most notably load and other time-varying unobservables captured via season-by-year fixed effects (ω_{sy}). The results from the Heckman two-step model discussed in the following section will allow us to quantify more precisely how changes in relative fuel prices and wind generation affect the extensive margin response.

C. *Changes in Observed Capacity Factors*

Beyond estimating marginal impacts along the intensive margin, we are also interested in a retrospective analysis to determine how the collapse in natural gas prices and increase in wind generation contributed to the recent decline in coal-fired generation and the extent to which those contributions vary across regions. More precisely, we want to isolate the impact that changing relative fuel prices and wind generation levels between 2008 and 2013 has had on the overall observed change in capacity factors between these two years, inclusive of both intensive and extensive margin responses.[17] In other words, if we abstract away from possible increasing regulatory scrutiny over the 2008 to 2013 period, would a 2008 environment—but with 2013 input prices and wind generation levels—have led to similar drops in

[17] We have also looked at how P^R and W observed changes over time have led to predicted changes in emissions per unit of capacity. The results are qualitatively similar to those presented below for capacity factor responses (see Figure C.6 in online Appendix C).

capacity factors as to what we actually observed over the 2008 to 2013 period? To undertake this analysis we use the parameters from our Heckman two-step estimation as this allows us to formally incorporate fuel price and wind generation impacts for both the extensive (on/off decision) and intensive (generation conditional on operating) margins. To see this, consider the conditional expected value of CsF_{it}, including both censored and uncensored values ($CF_{it} = 0$ and $CF_{it} > 0$), from the Heckman two-step model:

$$E\left[CF_{it} \mid \mathbf{X}_{it}, \mathbf{V}_{it}\right] = \Phi\left(\mathbf{V}_{it}\alpha\right)\left[\mathbf{X}_{it}\beta + \rho\,\lambda_{it}\right]. \tag{7}$$

Here, $\mathbf{X}_{it}$ represents the value of all variables in the intensity equation, including unit and time fixed effects, and $\mathbf{V}_{it}$ represents the value of all variables in the selection equation. Note, $\mathbf{X}_{it}$ and $\mathbf{V}_{it}$ are the same except $\mathbf{V}_{it}$ includes the exclusion restriction variables L_{it-l}. The first term $\Phi\left(\mathbf{V}_{it}\alpha\right)$ represents the estimated probability that unit i has a positive y_{it} value given the values of $\mathbf{V}_{it}$ and where α represents the parameters estimated from the selection equation. Thus, this term picks up extensive margin impacts. The second term $\left[\mathbf{X}_{it}\beta + \rho\,\lambda_{it}\right]$ is the conditional expectation of y_{it} based on estimates for β and ρ from the intensity equation, where λ_{it} is the estimated value of the inverse Mills ratio (IMR), and thus this term captures the intensive margin impacts. Note that while λ_{it} depends on $\mathbf{V}_{it}\alpha$ from the selection equation, the purpose of λ_{it} is to correct the intensive margin estimate, and as such, we consider the entire term in brackets to represent the intensive margin response.

To determine how much of the change in CF is due to changing P^R and W values, we first calculate the predicted value of y_{it}, replacing the P^R_{it} and/or W_t values in $\mathbf{X}_{it}$ and $\mathbf{V}_{it}$ in (7) with the 2013 average P^R and W values, denoted as $\overline{P}^R_{2013}$ and $\overline{W}_{2013}$, respectively. This gives counterfactual estimates of capacity factors under fuel prices or wind generation at 2013 average levels, but all else (i.e., load and season-year fixed effects) remaining as it was in 2008.[18] Once we have the predicted counterfactual CF_{it} values for capacity factors under 2013 average P^R or W values, we take the average of that prediction and subtract off the actual observed average 2008 CF_{it} values to obtain the predicted change in CF_{it} if P^R alone, W alone, or jointly P^R and W were at their 2013 average levels.[19] We then compare these predicted changes

[18] Note that substituting P^R and W affects the IMR term in (7). To construct a counterfactual IMR estimate, we first estimate a probit model of equation (3), inclusive of the unit fixed effects. Next, the parameter estimates from this probit model are used to predict the IMR under different values of P^R and W. Specifically, the estimated IMR is $\hat{\lambda}_{it} = \phi(\mathbf{V}_{it}\hat{\alpha})/\Phi(\mathbf{V}_{it}\hat{\alpha})$, where $\phi(\cdot)$ and $\Phi(\cdot)$ are the normal pdf and cdf, respectively, and $\hat{\alpha}$ is the vector of parameter estimates from the probit model. Unfortunately, this probit estimation with unit fixed effects will suffer the well-known incidental parameters problem. However, given the large-T sample, the bias is attenuated (Greene 2011) and thus this naïve method will still approximate the IMR well. Note the bias correction approach of Fernández-Val and Vella (2011) cannot be used because an IMR is required for every observation, not just those in the selected sample. However, when comparing the IMR derived from this naïve approach (with the observed $\mathbf{V}_{it}$) with the bias-corrected approach of Fernández-Val and Vella (2011) for the selected sample, the means and variances of these two IMR calculations in each region are quite similar.

[19] One concern is that inserting annual average values of P^R and W into their daily counterparts in the expectations equation (7) may obscure the expectation given seasonality and the nonlinearity of equation (7). However, substituting in $\overline{P}^R_{2013}$ and $\overline{W}_{2013}$ in equation (7) and then taking the average of the predicted expected CF_{it} values for 2013 gives an average predicted value that is very close to the observed average CF_{it} value in 2013, and similarly for 2008. The worst prediction across 2008 and 2013 is in PJM for 2013 where the predicted average capacity factor is 1.8 percent lower than the observed average (0.44 compared to 0.448). Differences between predicted and observed averages in other regions for both 2008 and 2013 were all below 1 percent of the observed average.

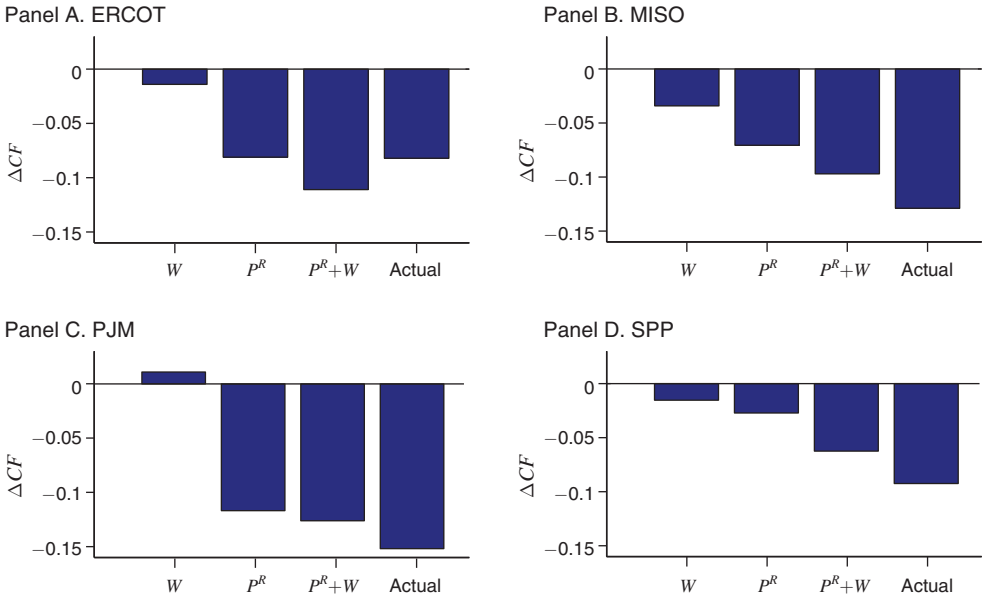

FIGURE 6. CAPACITY FACTOR CHANGE DECOMPOSITION

in capacity factor to the "actual" observed difference in average capacity factors between 2008 and 2013, which can be obtained by simply taking 2013 average *CF* values given in Table 1 minus the 2008 average *CF* values.

Figure 6 displays the predicted changes in capacity factor levels associated with wind being at the 2013 average level (W), P^R being at the 2013 average level (P^R), and wind and P^R both at their respective 2013 average levels $(P^R + W)$. The figure also shows the difference in observed average capacity factors between 2008 and 2013 (actual). Several key features of this figure are worth noting. First, across all regions, the change in P^R and W combined can explain the majority of the observed decline in average capacity factors, with $P^R + W$ predictions equal to 135 percent (ERCOT), 75 percent (MISO), 83 percent (PJM), and 68 percent (SPP) of observed changes in capacity factors.[20] Second, in all regions, changes in fuel prices had a larger impact alone on capacity factors than wind, likely due to the considerable increase in the coal-to-gas price ratio in these regions. Finally, highlighting the importance of the interaction effect, the sum of the W bar and the P^R bar is less than the $P^R + W$ bar (with the exception of MISO)—the percent difference

[20]The fact that actual averages fell less than predicted changes is possible for several reasons. For instance, in ERCOT load expanded from 2008 to 2013, which would counteract the negative impacts of increasing W and P^R values to some extent and make the "Actual" bars fall less than the "$P^R + W$" bar. Additionally, the estimated changes are based on 2008-counterfactual *CF*s that use 2008 season-year fixed effects, which may vary from the 2013 season-year fixed effects. In addition, to get a sense of the standard errors associated with these estimates we ran a blocked bootstrapped procedure with 1,000 iterations for each region. While the computational complexity of the problem allowed only for a relatively small number of iterations, the derived 95 percent confidence intervals for each regions' "$P^R + W$" predicted change spans the "Actual" average change in capacity factor and does not include zero. The bootstrap procedure also finds "P^R" and "W" predicted changes were different from zero at the 5 percent significance level in all regions except SPP.

between $P^R + W$ and the sum of W and P^R is 16.6 percent in ERCOT, -7.4 percent in MISO, 19.2 percent in PJM, and 46.7 percent in SPP.[21]

We also examine the relative contribution to the predicted changes in capacity factor from the intensive margin versus extensive margin responses. Recall from Table 8 that predicted propensity scores fell substantially in PJM and to a lesser extent in MISO, with smaller declines in ERCOT and SPP. Decomposing the responses from equation (7) yields a similar story. In ERCOT and MISO, the intensive margin response is roughly three times the extensive margin response, while in PJM the extensive margin response is quite a bit larger than in the other regions, and only slightly smaller in magnitude than the intensive margin response. SPP is more surprising, with a near-zero extensive margin response.[22]

As a final point, the estimates for SPP stand out for two reasons: the price response is substantially smaller than in other regions, and somewhat less of the total observed changes in capacity factors can be attributed to P^R and W changes. SPP did see the smallest change in average P^R levels over time across the four regions we examined, which may explain a smaller price response. Another key difference is that SPP was dominated by large integrated and regulated utilities over the time analyzed, whereas in the other regions, the majority of states had deregulated their electricity markets and broken up their integrated utilities. It is plausible that due to cost-of-service regulation and the relative infrequency of changes in electricity rates, integrated utilities may be less responsive on a day-to-day basis to contemporaneous fluctuations in fuel prices, compared to units operating in competitive wholesale electricity markets. However, over longer time spans, the integrated utilities may still respond to changes in relative fuel prices due to pressure from their regulators, but these longer term responses would be picked up by our time fixed effects instead of responses to daily P^R changes. In contrast, both deregulated wholesale markets and integrated utilities still must balance load and generation and thus could have similar daily responses to wind generation. Overall, this suggests the need for further research into the differences in fossil-fuel fired generation responses to fuel prices and renewable generation across regulated and deregulated electricity market regions.

IV. Conclusion

In the preceding sections, we examine the joint impact of the dramatic fall in natural gas prices and the substantial increase in wind generation on coal-fired generation and CO_2 emissions from 2008 to 2013. We find lower natural gas prices and increased wind generation have decreased coal-fired generation and emissions. Importantly though, we also find an effect not considered in related papers,

[21] In Figure C.5 in online Appendix C, we also plot the predicted changes in capacity factor with the interaction variable "turned off." With the exception of MISO, predicted changes in capacity factor are substantially smaller in magnitude, particularly in SPP.

[22] Details of how we calculate the attribution of extensive and intensive margin effects from the overall predicted change are given in online Appendix A. For each region, the percent of the total predicted change from 2008 observed average capacity factors assuming fuel prices and wind generation were at their 2013 averages is as follows: ERCOT—78 percent intensive, 22 percent extensive; MISO—74 percent intensive, 26 percent extensive; PJM—59 percent intensive, 41 percent extensive; SPP—94 percent intensive, 6 percent extensive.

specifically a statistically and economically significant interaction effect between fuel prices and wind generation in most regions. The interaction effect implies cheaper natural gas and greater wind generation levels together lead to a greater reduction in coal-fired generation and emissions than either factor in isolation. The magnitude of this interaction effect is substantial, and in some regions, marginal responses of coal-fired generation to wind generation in 2013 are several times what they would have been had natural gas prices remained at 2008 levels. Similar sensitivities are found for responses to relative fuel prices.

The quantile method employed allows an examination of heterogeneity in the response to wind generation and fuel prices across different quantiles, finding generally larger responses at lower quantiles. For example, marginal responses to wind at the twenty-fifth quantile were up to twice as large as for the seventy-fifth quantile. In PJM, the marginal response at the twenty-fifth quantile is surprisingly small, but this likely reflects technical constraints that would have restricted the ability of plants to turn-down further in response to relative fuel prices and wind generation without shutting off completely. Results are robust across a variety of alternative specifications and provide a nuanced examination of the intensive margin response of coal-fired plants to changing relative fuel prices and wind generation.

Using a modified Heckman two-step approach, counterfactual capacity factor levels under various fuel price ratios and wind generation levels from 2008 to 2013 are generated, capturing both intensive and extensive margin responses by coal-fired plants. Importantly, we find that falling natural gas prices combined with increased wind generation account for most of the observed decline in average coal capacity factors from 2008 to 2013, with predicted changes ranging from 68 to over 100 percent of observed changes. In ERCOT, MISO, and SPP, the intensive margin response is substantially larger than the extensive margin response, while PJM has more similar responses along the two margins. In addition, we find that falling gas prices had a larger impact than wind growth on capacity factors. Interestingly, SPP shows a smaller fuel price response than the other regions, possibly reflecting the fact that SPP at the time was dominated by large integrated utilities who may respond differently, or at least on different temporal scales, to fuel price changes than deregulated power plants.

Finally, although our analysis provides insight into the evolution of electricity sector operations over the last few years, as well as potential impacts of future policies, an important caveat is in order. While we focus on the short-run operating margin, there may be important effects of natural gas prices and wind generation growth on longer-run build decisions that warrant further inquiry.

REFERENCES

Baranes, Edmond, Julien Jacqmin, and Jean-Christophe Poudou. 2015. "Non-renewable and intermittent renewable energy sources: Friends and foes?" French Association of Environmental and Resource Economists (FAERE) Working Paper 2015.02.

Callaway, Duncan, Meredith Fowlie, and Gavin McCormick. 2015. "Location, location, location: The variable value of renewable energy and demand-side efficiency resources." Energy Institute at Haas Working Paper 264.

Cullen, Joseph. 2013. "Measuring the Environmental Benefits of Wind-Generated Electricity." *American Economic Journal: Economic Policy* 5 (4): 107–33.

Cullen, Joseph A., and Erin T. Mansur. 2017. "Inferring Carbon Abatement Costs in Electricity Markets: A Revealed Preference Approach Using the Shale Revolution." *American Economic Journal: Economic Policy* 9 (3): 106–33.

Denholm, Paul, Gerald L. Kulcinski, and Tracey Holloway. 2005. "Emissions and Energy Efficiency Assessment of Baseload Wind Energy Systems." *Environmental Science and Technology* 39 (6): 1903–11.

Dorsey-Palmateer, Reid. 2014. "Effects of Wind Power Intermittency on Generation and Emissions." www-personal.umich.edu/ reiddp/JMP.pdf.

Fell, Harrison, and Daniel T. Kaffine. 2018. "The Fall of Coal: Joint Impacts of Fuel Prices and Renewables on Generation and Emissions: Dataset." *American Economic Journal: Economic Policy.* https://doi.org/10.1257/pol.20150321.

Fell, Harrison, and Joshua Linn. 2013. "Renewable electricity policies, heterogeneity, and cost effectiveness." *Journal of Environmental Economics and Management* 66 (3): 688–707.

Fernández-Val, Iván. 2009. "Fixed effects estimation of structural parameters and marginal effects in panel probit models." *Journal of Econometrics* 150 (1): 71–85.

Fernández-Val, Iván, and Francis Vella. 2011. "Bias corrections for two-step fixed effects panel data estimators." *Journal of Econometrics* 163 (2): 144–62.

Galvao, Antonio F., Carlos Lamarche, and Luiz Renato Lima. 2013. "Estimation of Censored Quantile Regression for Panel Data With Fixed Effects." *Journal of the American Statistical Association* 108 (503): 1075–89.

Greene, William H. 2011. *Econometric Analysis.* 7th ed. London: Pearson.

Holladay, J. Scott, and Jacob LaRiviere. 2017. "The impact of cheap natural gas on marginal emissions from electricity generation and implications for energy policy." *Journal of Environmental Economics and Management* 85: 205–27.

Jenner, Steffen, and Alberto J. Lamadrid. 2013. "Shale gas vs. coal: Policy implications from environmental impact comparisons of shale gas, conventional gas, and coal on air, water, and land in the United States." *Energy Policy* 53: 442–53.

Joskow, Paul L. 2011. "Comparing the Costs of Intermittent and Dispatchable Electricity Generating Technologies." *American Economic Review* 101 (3): 238–41.

Joskow, Paul L. 2013. "Natural Gas: From shortages to abundance in the United States." *American Economic Review* 103 (3): 338–43.

Kaffine, Daniel T., Brannin J. McBee, and Jozef Lieskovsky. 2013. "Emissions Savings from Wind Power Generation in Texas." *Energy Journal* 34 (1): 155–75.

Knittel, Christopher R., Konstantinos Metaxoglou, and Andre Trindade. 2015. "Natural Gas Prices and Coal Displacement: Evidence from Electricity Markets." National Bureau of Economic Research (NBER) Working Paper 21627.

Linn, Joshua, Erin Mastrangelo, and Dallas Burtraw. 2014. "Regulating Greenhouse Gases from Coal Power Plants under the Clean Air Act." *Journal of the Association of Environmental and Resource Economists* 1 (1–2): 97–134.

Linn, Joshua, Lucija Anna Muehlenbachs, and Yushuang Wang. 2014. "How Do Natural Gas Prices Affect Electricity Consumers and the Environment?" Resources for the Future Working Paper 14–19.

Lu, Xi, Jackson Salovaara, and Michael B. McElroy. 2012. "Implications of the Recent Reductions in Natural Gas Prices for Emissions of CO2 from the US Power Sector." *Environmental Science and Technology* 46 (5): 3014–21.

Muller, Nicholas Z., and Robert Mendelsohn. 2009. "Efficient Pollution Regulation: Getting the Prices Right." *American Economic Review* 99 (5): 1714–39.

Newcomer, Adam, Seth A. Blumsack, Jay Apt, Lester B. Lave, and M. Granger Morgan. 2008. "Short Run Effects of a Price on Carbon Dioxide Emissions from U.S. Electric Generators." *Environmental Science and Technology* 42 (9): 3139–44.

Novan, Kevin M. 2015. "Valuing the Wind: Renewable Energy Policies and Air Pollution Avoided." *American Economic Journal: Economic Policy* 7 (3): 291–326.

Powell, J. L. 1986. "Censored Regression Quantiles." *Journal of Econometrics* 32 (1): 143–55.

Schmalensee, Richard. 2012. "Evaluating Policies to Increase Electricity Generation from Renewable Energy." *Review of Environmental Economics and Policy* 6 (1): 45–64.

This article has been cited by:

1. Lili Ding, Zhongchao Zhao, Meng Han. 2021. Probability density forecasts for steam coal prices in China: The role of high-frequency factors. *Energy* 119758. [Crossref]
2. Harrison Fell, Jeremiah X. Johnson. 2020. Regional disparities in emissions reduction and net trade from renewables. *Nature Sustainability* **5**. . [Crossref]
3. Kelly A. Stevens, Deborah A. Carroll. 2020. A comparison of different carbon taxes on utilization of natural gas. *Energy and Climate Change* **1**, 100005. [Crossref]
4. Klaus Gugler, Adhurim Haxhimusa, Mario Liebensteiner. 2020. Effectiveness of climate policies: Carbon pricing vs. subsidizing renewables. *Journal of Environmental Economics and Management* 102405. [Crossref]
5. Xinde Ji, Kelly M. Cobourn. 2020. Weather Fluctuations, Expectation Formation, and Short-Run Behavioral Responses to Climate Change. *Environmental and Resource Economics* **49**. . [Crossref]
6. J. Mijin Cha. 2020. A just transition for whom? Politics, contestation, and social identity in the disruption of coal in the Powder River Basin. *Energy Research & Social Science* **69**, 101657. [Crossref]
7. Stephen P. Holland, Erin T. Mansur, Nicholas Z. Muller, Andrew J. Yates. 2020. Decompositions and Policy Consequences of an Extraordinary Decline in Air Pollution from Electricity Generation. *American Economic Journal: Economic Policy* **12**:4, 244-274. [Abstract] [View PDF article] [PDF with links]
8. Alex Perez, John J. Garcia-Rendon. 2020. Integration of non-conventional renewable energy and spot price of electricity: A counterfactual analysis for Colombia. *Renewable Energy* . [Crossref]
9. John E.T. Bistline, Maxwell Brown, Sauleh A. Siddiqui, Kathleen Vaillancourt. 2020. Electric sector impacts of renewable policy coordination: A multi-model study of the North American energy system. *Energy Policy* **145**, 111707. [Crossref]
10. Rui Shan, Colin Sasthav, Xianxun Wang, Luana M.M. Lima. 2020. Complementary relationship between small-hydropower and increasing penetration of solar photovoltaics: Evidence from CAISO. *Renewable Energy* **155**, 1139-1146. [Crossref]
11. Jonathan E. Hughes, Ian Lange. 2020. WHO (ELSE) BENEFITS FROM ELECTRICITY DEREGULATION? COAL PRICES, NATURAL GAS, AND PRICE DISCRIMINATION. *Economic Inquiry* **58**:3, 1053-1075. [Crossref]
12. J. Zarnikau, C.H. Tsai, C.K. Woo. 2020. Determinants of the wholesale prices of energy and ancillary services in the U.S. Midcontinent electricity market. *Energy* **195**, 117051. [Crossref]
13. Konstantinos Metaxoglou, Aaron Smith. 2020. Productivity Spillovers From Pollution Reduction: Reducing Coal Use Increases Crop Yields. *American Journal of Agricultural Economics* **102**:1, 259-280. [Crossref]
14. James H. Stock. 2020. Climate Change, Climate Policy, and Economic Growth. *NBER Macroeconomics Annual* **34**, 399-419. [Crossref]
15. Matteo Di Castelnuovo, Andrea Biancardi. The Future of Energy Infrastructure 5-52. [Crossref]
16. Joshua Linn, Kristen McCormack. 2019. The roles of energy markets and environmental regulation in reducing coal-fired plant profits and electricity sector emissions. *The RAND Journal of Economics* **50**:4, 733-767. [Crossref]
17. Paul Brehm. 2019. Natural gas prices, electric generation investment, and greenhouse gas emissions. *Resource and Energy Economics* **58**, 101106. [Crossref]

18. Kristina Mohlin, Alex Bi, Susanne Brooks, Jonathan Camuzeaux, Thomas Stoerk. 2019. Turning the corner on US power sector CO 2 emissions—a 1990–2015 state level analysis. *Environmental Research Letters* **14**:8, 084049. [Crossref]
19. Zsuzsanna Csereklyei, Songze Qu, Tihomir Ancev. 2019. The effect of wind and solar power generation on wholesale electricity prices in Australia. *Energy Policy* **131**, 358-369. [Crossref]
20. Reid Dorsey-Palmateer. 2019. Effects of wind power intermittency on generation and emissions. *The Electricity Journal* **32**:3, 25-30. [Crossref]
21. Alessio Saretto, Anastasia Shcherbakova, Jeremy Lin. 2019. Marginal Fuel Switching and Price Volatility in PJM. *SSRN Electronic Journal* . [Crossref]
22. Philip Schnaars. 2019. The Real Substitution Effect of Renewable Electricity: An Empirical Analysis for Germany. *SSRN Electronic Journal* . [Crossref]
23. Yiyi Bai, Samuel J Okullo. 2019. Cutting Carbon Through Fuel-Switching Under the EU ETS. *SSRN Electronic Journal* . [Crossref]
24. Hei Sing Chan, Yichen Zhou. 2019. Regulatory Spillover and Climate Co-Benefits: Evidence from the New Source Review Lawsuits. *SSRN Electronic Journal* . [Crossref]
25. Joshua Linn, Lucija Muehlenbachs. 2018. The heterogeneous impacts of low natural gas prices on consumers and the environment. *Journal of Environmental Economics and Management* **89**, 1-28. [Crossref]
26. Matthew Doyle, Harrison Fell. 2018. Fuel prices, restructuring, and natural gas plant operations. *Resource and Energy Economics* **52**, 153-172. [Crossref]
27. Jeremy Weber. 2018. On Environmental Policy and Jobs: An Analogy with Trade and an Illustration with Coal. *SSRN Electronic Journal* . [Crossref]